Printed ISSN 1330–0008
Online ISSN 1333–9125
CD ISSN 1333–8390
CODEN FIZAE4

DEPOLARIZATION CROSSOVERS IN THE MICROWAVE RESPONSE OF SILICON CRYSTALS IN SLAB GEOMETRY

BAKIR BABIĆ [a], MARIO BASLETIĆ [b], ANTONIJE DULČIĆ [b] and MIROSLAV POŽEK [b]

[a] *ETH Hönggerberg, Institute of Quantum Electronics, CH-8093 Zürich, Switzerland*

[b] *Department of Physics, Faculty of Science, POB 331, HR-10001 Zagreb, Croatia*

Dedicated to the memory of Professor Zvonko Ogorelec

Received 28 September 2004; Accepted 31 January 2005
Online 10 November 2006

Microwave cavity perturbation measurements have been performed on several n-type silicon samples with different depolarization factors due to sample geometries. The general solution for the complex frequency shift in slab geometry is discussed for the specific case of semiconductors. The depolarization crossovers predicted by the theory have been experimentally observed. Their relative intensities suggest that the imaginary part of the complex conductivity of semiconductors has to be taken into account. Electron scattering time has been inferred from the microwave measurements.

PACS numbers: 72.30.+q, 72.80.Cw, 72.20.-i UDC 537.86, 537.311.6

Keywords: n-type silicon, slab geometry, microwave measurement, complex frequency shift, depolarization factors, electron scattering time

1. Introduction

Investigation of samples with variable dielectric, magnetic or conducting properties at microwave frequencies is very useful for the determination of their material parameters. Microwave experiments based on resonant cavities or other resonant structures are widely used since they offer the best signal/noise ratios. Usually, a small sample is introduced into a microwave cavity as a perturbation. The measured quantities are changes of the Q-factor and the resonant frequency of the cavity, combined in a single complex quantity named complex frequency shift. In our recent paper[1], we have developed a general solution for the complex frequency shift of a resonant cavity perturbed by a small sample with a slab geometry. Although the solution is general for samples with different electric and magnetic properties, the experimental verification and analysis given in Ref. [1] was restricted to superconducting films.

Semiconductors, with their huge changes in conductivity with temperature, offer a suitable system to check the validity of the general solution. If the proper sample thickness and geometry is chosen, the sample should change from effectively insulating to conducting regime. In the microwave response, one may expect two depolarization crossovers in the temperature range $4-300$ K. In this paper, we provide the experimental verification of the validity of the general solution [1] using silicon samples whose conductivities vary with temperature over several orders of magnitude.

2. *Complex frequency shift*

In a cavity loaded with a sample, losses occur in the cavity walls and in the sample. They can be represented by introducing the time dependence of the fields in a form $\exp(i\tilde{\omega}t)$, where $\tilde{\omega} = \omega(1 + \mathrm{i}/2Q)$ is the complex frequency which includes losses through the Q-factor of the cavity. Generally, one is interested in the change of $\tilde{\omega}$

$$\frac{\Delta\tilde{\omega}}{\omega} = \frac{\Delta f}{f} + \mathrm{i}\Delta\left(\frac{1}{2Q}\right), \tag{1}$$

due to the changes of sample properties while keeping the losses in the cavity walls constant. It is readily achieved if the cavity temperature is fixed and if the sample volume is small compared to the cavity volume. Under these conditions, the complex frequency shift is given by the surface integral over the sample surface [1]

$$\frac{\delta\widetilde{\omega}_{\mathrm{p}}}{\omega} = \frac{\mathrm{i}}{\omega \mathrm{W_c}} \oint\limits_{\mathrm{S_s}} [\mathbf{E}^* \times \delta\mathbf{H} - \mathbf{H}^* \times \delta\mathbf{E}] \cdot \mathbf{n}_{\mathrm{s}} \mathrm{d}S\,, \tag{2}$$

where W_c is the energy stored in the cavity, and $\mathbf{n_s}$ is the unit vector normal to the sample surface and points into the sample. Therefore, for the determination of the complex frequency shift it suffices to determine electric and magnetic fields at the surface.

If the sample is platelike and placed in the maximum of the microwave electric field, the field solutions for the slab geometry may serve as a good approximation

$$\widetilde{E}(z) = \widetilde{E}_s \frac{\cosh(\mathrm{i}\widetilde{k}z)}{\cosh(\mathrm{i}\widetilde{k}d/2)}\,, \tag{3}$$

$$\widetilde{B}(z) = \frac{\widetilde{k}}{\omega}\widetilde{E}_s \frac{\sinh(\mathrm{i}\widetilde{k}z)}{\cosh(\mathrm{i}\widetilde{k}d/2)}\,, \tag{4}$$

where d is the thickness of the slab, $\widetilde{E}_s = \widetilde{E}(d/2)$ is the field at the surface. $\widetilde{k}$ is the complex wave vector given by

$$\widetilde{k} = k_0 \sqrt{\widetilde{\mu}_r \left(\widetilde{\epsilon}_r - \mathrm{i} \frac{\widetilde{\sigma}}{\epsilon_0 \omega} \right)} \,, \tag{5}$$

where $k_0 = \omega\sqrt{\mu_0 \epsilon_0}$ is the vacuum wave vector. The complex wave vector describes generally any set of material parameters.

It is, however, nontrivial to relate surface fields of Eqs. (3) and (4) with the driving field E_0. The problem can be solved in the quasistatic limit with an effective complex dielectric permitivity $\widetilde{\epsilon}_s$. One has to take into account the finite width and length of the sample in addition to its thickness. The geometry effect is introduced through the depolarization factor N. It was shown that the relation between the surface field $\widetilde{E}_s$ and the driving field E_0 is given by

$$\widetilde{E}_s = \frac{E_0}{1 + (\widetilde{\epsilon}_\mathrm{s} - 1)\, N} \,, \tag{6}$$

where the complex valued $\widetilde{\epsilon}_s$ is given by

$$\widetilde{\epsilon}_s = \frac{\widetilde{k}^2}{\widetilde{\mu}_r k_0^2} \frac{\tanh(\mathrm{i}\widetilde{k}d/2)}{\mathrm{i}\widetilde{k}d/2} \,. \tag{7}$$

If one takes an idealized perfect conductor as the initial state of the sample, the complex frequency shift to an arbitrary state is given by

$$\frac{\Delta\widetilde{\omega}_p}{\omega} = \frac{\Gamma}{N} \left[1 + \left(\frac{\widetilde{k}^2}{k_0^2} \frac{\tanh(\mathrm{i}\widetilde{k}d/2)}{\mathrm{i}\widetilde{k}d/2} - 1 \right) N \right]^{-1} \,, \tag{8}$$

where Γ is the dimensionless filling factor of the sample in the cavity. Up to now, the consideration was quite general for any type of material.

In the remainder of the paper, we shall consider this general result for the case of a platelike semiconductor. Let us consider a model sample − a piece of a semiconductor similar to those which have been used in our experiments. We set $\epsilon_r = 12$, close to the value of silicon. Typical geometry of the sample was $d = 0.2$mm, $L_y = 2$mm and $L_x = 1$mm. Approximating the sample by an ellipsoid, the depolarization factor can be calculated using an integral [2]

$$N_\mathrm{e} = N_{L_y} = \frac{L_x L_y d}{2} \int\limits_0^\infty \frac{\mathrm{d}s}{\left(s + L_y^2\right) \sqrt{\left(s + {L_x}^2\right) \left(s + {L_y}^2\right) \left(s + d^2\right)}}, \tag{9}$$

which can be evaluated numerically. For the given geometry, its value is $N = 0.054$. For a sample with this geometry, we plot in Fig. 1a and b the imaginary and real

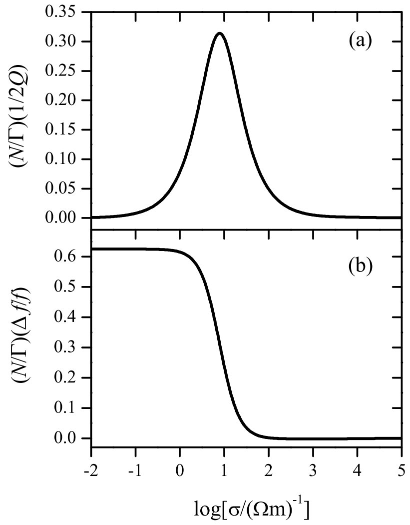

Fig. 1. Imaginary (a) and real (b) parts of the complex frequency shift as functions of the conductivity.

parts of the complex frequency shift. The salient feature is the depolarization peak observed in the imaginary part of $\Delta(1/2Q)$. It marks the crossover from practically insulating to conducting regime of the semiconductor. The position of the peak depends on the depolarization factor N of the particular sample and is given by the condition $\sigma^* \approx [1 + (\epsilon_r - 1)N]\epsilon_0\omega/N$.

3. Conductivity of silicon

Semiconducting samples change their conductivity by several orders of magnitude in the temperature range from 4 K to the room temperature. It is of interest to analyze a simulated complex frequency shift due to a model semiconductor sample. In the present case, we use n-type silicon samples with $E_g = 1.12\,\mathrm{eV}$, $E_d = 0.044\,\mathrm{eV}$, $m_e = 0.40m$ and $m_h = 0.41m$ [3]. The conductivity is given by

$$\sigma(T) = e\mu_e(T)n(T) \ , \tag{10}$$

where $n(T)$ is the electron concentration given by [4]

$$\begin{aligned} n(T) \quad &= \quad \frac{1}{4}\left[\left(-N_c(T)e^{-E_d/kT}\right) + \sqrt{\left(N_c(T)e^{-E_d/kT}\right)^2 + 8N_dN_c(T)e^{-E_d/kT}}\right] \\ &+ \quad n_i(T)e^{-E_g/2kT} \ . \end{aligned} \tag{11}$$

The temperature dependence of the mobility $\mu_e(T)$ is determined by the scattering time τ. We assume that in the saturation regime and at higher temperatures, electron-phonon scattering dominates and the mobility is then given by $\mu_e(T) = AT^{-3/2}$, where the constant A is determined from the conductivity at room temperature. Our model sample has a donor concentration $N_d = 2 \cdot 10^{20}\mathrm{m}^{-3}$ and the room temperature conductivity $\sigma(270\,\mathrm{K}) = 10\ \Omega^{-1}\mathrm{m}^{-1}$. The conductivity $\sigma(T)$ can be readily calculated, and Fig. 2a shows the logarithm of conductivity vs. $1/T$ for given parameters. Fig. 2b shows the same conductivity vs. T in the temperature range up to the room temperature. If this conductivity is inserted in Eq. (8), for a sample with $d = 0.2$mm and $N = 0.054$ (the same as in Fig. 1), one obtains the temperature dependence of the imaginary and real parts of the complex frequency shift shown in Fig. 3. The depolarization crossover occurs when the

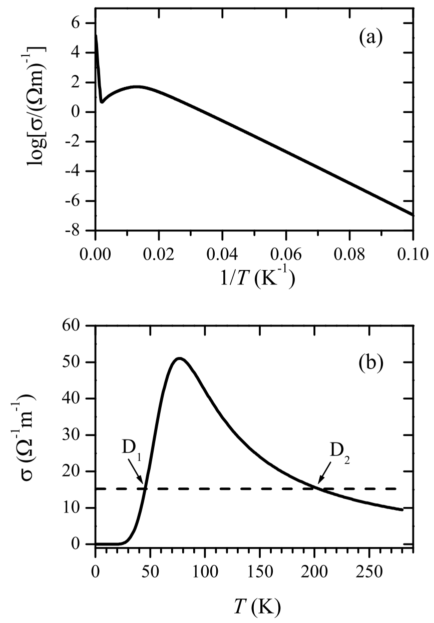

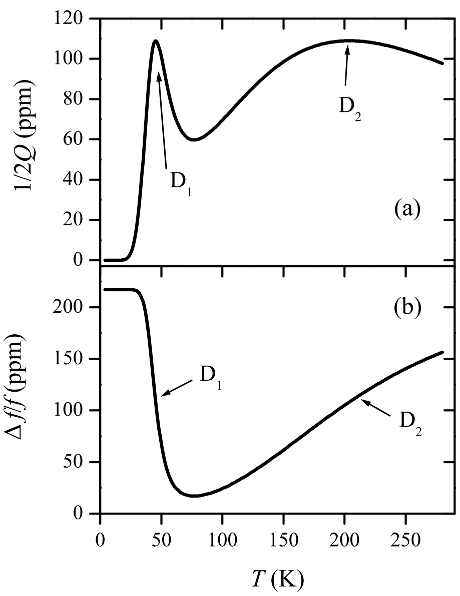

Fig. 2 (left). Temperature dependence of the conductivity calculated from Eqs. (10) and (11) for a silicon sample with donor concentration $N_d = 2 \cdot 10^{20}\mathrm{m}^{-3}$ and conductivity $\sigma(270\mathrm{K}) = 10\Omega^{-1}\mathrm{m}^{-1}$. The dashed line indicates the conductivity σ^* where depolarization crossover is expected in the microwave response.

Fig. 3. Temperature dependence of the complex frequency shift of a silicon sample with conductivity shown in Fig. 2 and geometry parameters as in Fig. 1. The two depolarization crossovers are indicated in compliance with Fig. 2.

conductivity crosses the value $\sigma^* \approx [1 + (\epsilon_r - 1)N]\epsilon_0\omega/N = 15.21\,\Omega^{-1}\mathrm{m}^{-1}$. This value is indicated as a dashed line in Fig. 2b. Therefore, one expects two depolarization crossovers. The sample is first crossing σ^* as the conductivity increases due to the ionization of donor levels. This crossover yields the low-temperature peak of $1/2Q$ in Fig. 3. When the conductivity in Fig. 2 reaches its maximum, the decrease of $1/2Q$ in Fig. 3 stops. At higher temperatures, the number of carriers is saturated and the conductivity is lowered due to the increased phonon scattering. The sample crosses again to the insulating side at σ^*. This is seen as a broad maximum of $1/2Q$ in Fig. 3. Of course, one would expect the third crossover at much higher temperatures when the carrier concentration increases due to the intrinsic ionization.

4. Experimental results

In this section we shall describe experimental demonstrations of some features discussed in the preceeding sections. We have cut the samples from three different commercially obtained wafers of n-type silicon. Wafer A had a nominal concentration of donors $N_d \approx 6 \times 10^{20}\mathrm{m}^{-3}$ and the conductivity $\sigma(270\,\mathrm{K}) \approx 16\,\Omega^{-1}\mathrm{m}^{-1}$. Wafer B had a nominal concentration of donors $N_d \approx 1.5 \times 10^{20}\mathrm{m}^{-3}$ and the conductivity $\sigma(270\,\mathrm{K}) \approx 5\,\Omega^{-1}\mathrm{m}^{-1}$. Wafer C had a nominal concentration of donors $N_d \approx 4 \times 10^{19}\mathrm{m}^{-3}$ and the conductivity $\sigma(270\,\mathrm{K}) \approx 1\,\Omega^{-1}\mathrm{m}^{-1}$. DC conductivities of wafers A and C have been measured by a four-contact method in the temperature range from 77 K to 290 K. They can be well fitted by Eqs. (10) and (11) if the temperature dependence of the mobility is assumed to be $\mu_e(T) = AT^{-1.8}$.

For the microwave measurements, samples were cut out from the wafers. Table 1. lists dimensions of all pieces that were measured, together with the depolarization factors calculated using Eq. (9).

TABLE 1. Geometric parameters of the samples used in the microwave measurements.

Wafer	Length (mm)	Width (mm)	d (mm)	N
A	1.7	1.1	0.16	0.057
	1.9	1.6	0.25	0.084
	1.8	1.6	0.25	0.089
	2.2	1.0	0.45	0.093
	2.3	1.9	0.45	0.115
B	1.9	0.7	0.15	0.038
	1.9	1.2	0.22	0.068
	1.7	0.8	0.4	0.104
	1.9	1.2	0.4	0.110
	1.7	0.8	0.6	0.137
C	1.8	1.6	0.25	0.085

An elliptical copper cavity resonating in the $_{\mathrm{e}}\mathrm{TE}_{111}$ mode at ≈ 9.3GHz was used. The samples were mounted on a sapphire holder in the centre of the cavity, along the microwave electric field. We used a BRUKER microwave bridge operating at 9 – 10 GHz. The Q factor was measured by a modulation technique described elsewhere [5, 6]. The empty cavity absorption ($1/2Q$) was substracted from the measured data and the presented experimental curves are due to the samples themselves. An automatic frequency control (AFC) system was used to track the klystron frequency so as to keep it always in resonance with the cavity. Thus, the frequency shift can be measured as the temperature of the sample is varied.

Figure 4 shows the temperature dependence of absorption ($1/2Q$) and real frequency shift ($\Delta f/f$) of a silicon sample from wafer B with $d = 0.4$ mm and $N = 0.104$. One can clearly observe two depolarization crossovers. However, a closer insight reveals two distinctions with respect to the simulations given in Fig. 3. First, the height of the absorption peaks is not equal at the two crossovers in Fig. 4. If the absorption were determined by a single real parameter (σ), one would expect equal heights of the two peaks as shown in Fig. 3a. The real part of the frequency shift also shows a difference with respect to the shape shown in Fig. 3b. A small maximum in the real frequency shift occurs at a temperature just below the first crossover.

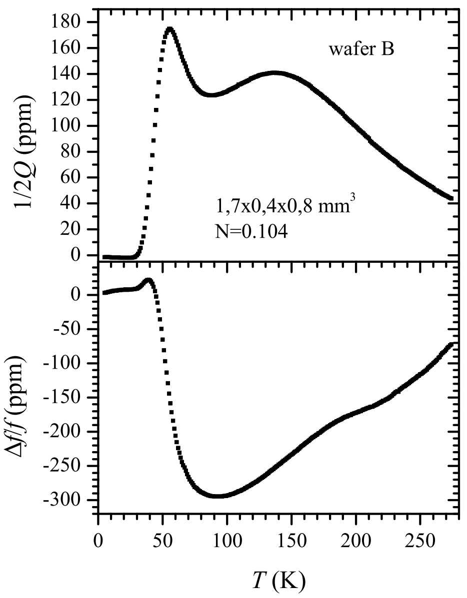

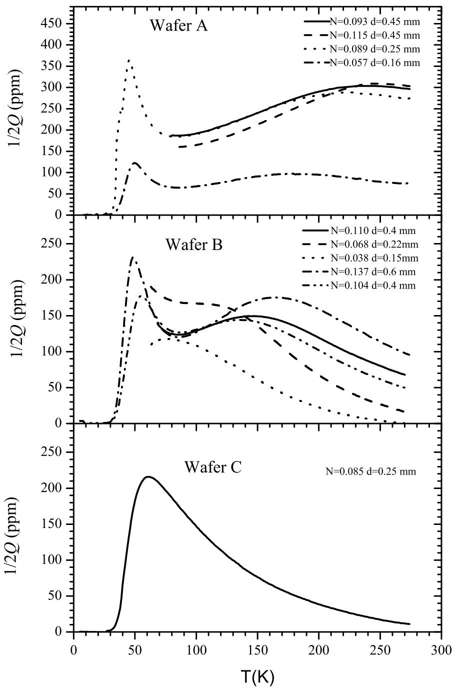

Fig. 4 (left). Measured complex frequency shift of a silicon sample from wafer B with $d = 0.4$ mm and $N = 0.104$.

Fig. 5. Measured imaginary parts of complex frequency shift of all samples.

Figure 5 shows the measured imaginary parts ($1/2Q$) of the complex frequency shifts for all sample pieces. Clearly, the positions of the depolarization peaks and their relative intensities strongly depend on the sample thicknesses d and static depolarization factors N. Furthermore, the intensity of the low-temperature peak is always higher than that of the high-temperature one for the same sample. Two of the samples even don't show the depolarization crossover (the thinnest sample of wafer B and the sample of wafer C). They never reach the crossover condition for σ^*, and stay at the insulating side of the depolarization crossover in the whole measured temperature range.

5. Discussion

In order to explain the features observed in Fig. 4, one has to introduce one more parameter that defines the shape of a complex frequency shift. For the purpose of simulation in Fig. 3, the conductivity was taken as a real quantity, implying that the current density and the electric field are in phase. However, the observations in Fig. 4 suggest that the microwave conductivity of the semiconductor could not be treated as a real quantity in the whole temperature range. Although the DC conductivity is the same at $\approx$ 140 K and at $\approx$ 50 K, the concentration of carriers is very different. Smaller concentration of carriers at 50 K is compensated by a larger mobility since the scattering time becomes larger. When the scattering time

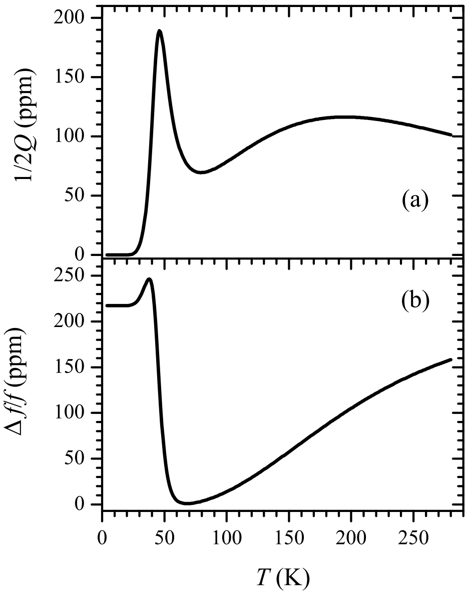

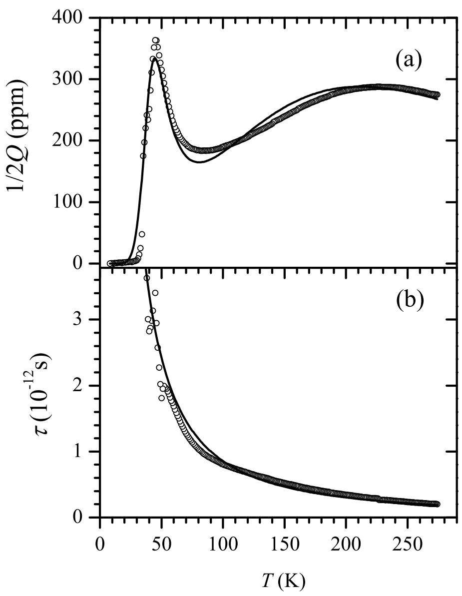

Fig. 6 (left). Complex frequency shift of the model sample calculated using the complex conductivity as explained in the text.

Fig. 7. (a) Measured imaginary part of the complex frequency shift (circles) and the fit with $\tau = 2.92 \cdot 10^{-12}\, T^{-3/2}\, \mathrm{s\,K^{-1}}$ (line); (b) Scattering time evaluated from the measurement (circles) and the fit with $\tau = 2.92 \cdot 10^{-12}\, T^{-3/2}\, \mathrm{s\,K^{-1}}$ (line).

becomes comparable to the period of the driving microwave field, i.e. $\tau\omega \approx 1$, the conductivity has to be treated as a complex quantity. It can be written in the form[7]

$$\widetilde{\sigma}(\omega) = \sigma(0)\frac{1 - \mathrm{i}\omega\tau}{1 + (\omega\tau)^2} \ . \tag{12}$$

We can calculate the values of $\tau\omega$ for our model sample described in Sect. 3. At the temperatures of absorption peaks, we obtain $\omega\tau(197\,\mathrm{K}) \approx 0.07$ and $\omega\tau(46\,\mathrm{K}) \approx 0.59$. Therefore, while the imaginary part of the conductivity is negligible at higher temperatures, it brings about a considerable contribution to the absorption amplitude at the low-temperature peak. Figure 6 shows the complex frequency shift of the model sample when the complex conductivity with $\tau \propto T^{-3/2}$ is taken into account. Qualitatively, one can see that all observed features from Fig. 4 can be reproduced in that way, especially the difference in amplitudes of the absorption peaks, and the existence of a small peak in the real part of the complex frequency shift at low temperatures.

For a real sample, one can deduce the scattering rate of the carriers from the shape of the microwave signal. For example, the signal of the sample from wafer A with $d = 0.25\,\mathrm{mm}$ and $N = 0.089$ can be well fitted with $\tau = 2.92{\cdot}10^{-12}\,T^{-3/2}\,\mathrm{s\,K}^{-1}$ as shown in Fig. 7a. It is also possible to use the experimental data and Eq. (8) to solve numerically for $\widetilde{\sigma}$, and then evaluate the scattering time τ. Figure 7b shows the results compared with the function used in the fit in Fig. 7a. Some discrepancy is noticed at lower temperatures indicating that phonon scattering alone cannot account for the complete scattering process.

6. Conclusions

We have analysed the cavity perturbation due to a semiconducting sample. The formula for the complex frequency shift [1] may predict the signal shapes for samples whose conductivities vary for several orders of magnitude, from insulating to conducting. The signal shapes depend not only on the conductivity, but also on the geometric parameters. We have demonstrated that the correct interpretation of signal shapes requires a complex conductivity at lower temperatures. It is achieved when the scattering rate in semiconductors becomes comparable with the period of the driving microwave field. In such cases, the present technique is suitable for the determination of the scattering rate.

Acknowledgements

Part of this work was conducted for the Diploma thesis of Bakir Babić in 2000. During this period, Bakir Babić had conducted very encouraging and fruitful discussions with late Professor Ogorelec. He is very thankful for those discussions.

The authors thank B. Pivac for providing the silicon wafers for the measurements.

References

[1] D.-N. Peligrad, B. Nebendahl, M. Mehring, A. Dulčić, M. Požek and D. Paar, Phys. Rev. B **64** (2001) 224504.

[2] C. J. F. Böttcher, *Theory of Electric Polarization*, Vol. 1, Second Edition, Elsevier, Amsterdam (1973).

[3] R. A. Smith, *Semiconductors*, Cambridge University Press, London, New York, Melbourne (1977).

[4] B. Sapoval and C. Hermann, *Physics of Semiconductors*, Springer-Verlag, New York (1995).

[5] B. Nebendahl, D.-N. Peligrad, M. Mehring, M. Požek and A. Dulčić, Rev. Sci. Instrum. **72** (2001) 1876.

[6] B. Nebendahl, Ph.D. Thesis, Universität Stuttgart (2004).

[7] K. Seeger, *Semiconductor Physics*, Springer, Berlin (1999).

DEPOLARIZACIJSKI PRIJELAZI U MIKROVALNOM ODZIVU PLOČICA SILICIJSKOG KRISTALA

Načinili smo mjerenja učinka umetanja nekoliko silicijskih pločica tipa n u mikrovalni rezonator s različitim depolarizacijskim faktorima uzrokovanim oblikom pločica. Raspravljamo opće rješenje za kompleksan pomak frekvencije za poseban slučaj poluvodičke pločice. Teorijski predviđene depolarizacijske prijelaze smo eksperimentalno opazili. Njihove relativne jakosti ukazuju da se u poluvodičima mora uzeti u obzir imaginarni dio kompleksne vodljivosti. Na osnovi mikrovalnih mjerenja izveli smo vrijeme elektronskog raspršenja.